Soil Dynamics and Earthquake Engineering 43 (2012) 261–270

Contents lists available at SciVerse ScienceDirect

Soil Dynamics and Earthquake Engineering

journal homepage: www.elsevier.com/locate/soildyn

Energy dissipation by nonlinear soil strains during soil–structure interaction excited by SH pulse

Vlado Gičev [a], Mihailo D. Trifunac [b,*]

[a] University of Goce Delčev, Department of Computer Science, Tošo Arsov 14, 2000 Štip, Republic of Macedonia
[b] University of Southern California, Department of Civil Engineering, Los Angeles, CA 90089-2531, USA

ARTICLE INFO

Article history:
Received 31 July 2011
Received in revised form
16 May 2012
Accepted 8 July 2012

ABSTRACT

Three variants of a two-dimensional (2-D) model of a building supported by a rectangular, flexible foundation embedded in nonlinear soil are analyzed. The building, the foundation, and soil have different physical properties. The building is assumed to be linear, but the foundation and the soil can experience nonlinear deformations. It is shown that the work spent for the development of nonlinear strains in the soil can consume a significant part of the input wave energy, and thus less energy is available for excitation of the building. The results help explain why the damage, during the 1994 Northridge earthquake in California, to residential buildings in the areas that experienced large strains in the soil was absent or reduced.

1. Introduction

Almost complete spatial separation of damaged buildings and of pipe breaks in the near field following the 1994 Northridge [45] and the 1933 Long Beach, California [36] earthquakes has brought out the need to understand the nature of nonlinear response of soils near the ground surface and its relationship to the soil–structure interaction (SSI). The absence of damaged buildings in the heavily shaken areas, where soil experienced large nonlinear strains and deformations, suggests the capacity of some soils to absorb the energy of incident seismic waves, and thus to act as a large-scale natural isolation system. Since the areas where this energy absorption takes place did recur during two consecutive earthquakes [46], the associated nonlinear phenomena appear to be associated with the local site characteristics, which do not change for decades, and which therefore should be used, with essentially no additional cost, in the design of individual structures and in the more advanced approaches to seismic zoning [38].

The zones where buildings were damaged during the 1994 Northridge earthquake, or where pipes were broken [42,43], are not associated with obvious and easily identifiable differences in the amplitudes of recorded peak accelerations [52], peak velocities [53], or spectral amplitudes of strong ground motion [30,31], and more subtle and detailed site investigations are required to identify them. These investigations will require detailed and multi-parametric site characterizations that combine the physical properties of the site with the level of its water table and liquefaction susceptibility [32,33,35,38]. The classical earthquake engineering approach correlates damage of structures with the largest relative response of the equivalent single-degree-of-freedom system, in a formulation that is typically based only on the largest relative peak of response [55]. While this approach can be refined to involve many largest peaks of the relative response [16,17] in the near field of strong ground shaking, it appears that the damage is more governed by the strong pulses that emanate from the broken asperities on the moving fault, and hence by the power of these pulses and the energy those pulses carry [37,11–13]. Therefore, we select for our studies the excitation in terms of simple pulses, to simulate the actions of strong ground motion near faults.

Following the early observational studies, which correlated the site properties with damage to typical residential buildings (like traditional wood houses in Japan) [6,22], studies of nonlinear response of soils to incident earthquake waves have focused on the changes in peak amplitudes of ground motion [4,41,57] and the changes in the site periods [39,40,47]. To understand how the energy of incident waves is absorbed during passage of large, near-field pulses it is necessary to work with hysteretic models of soils and to consider nonlinear representations of wave motion, which allow creation of strain-localization zones in the soil. To begin to understand these phenomena, we have started to analyze such problems incrementally in terms of simple models based on numerical modeling of two-dimensional SH wave motion and bilinear representation of nonlinear deformations [14]. We first considered nonlinear deformations in the soil and

* Corresponding author. Tel.: +1 213 740 0570; fax: +1 213 744 1426.
E-mail address: trifunac@usc.edu (M.D. Trifunac).

0267-7261/$ - see front matter © 2012 Elsevier Ltd. All rights reserved.
http://dx.doi.org/10.1016/j.soildyn.2012.07.008

relative energy absorption during 2-D SSI, when the foundation and the building are assumed to respond as continuous linear media [15]. In this paper, we continue and extend such analyses to (a) nonlinear soil and foundation, and (b) nonlinear soil and foundation, with a thin, soft layer having low yielding strain and surrounding the foundation, in both cases with the building responding in the linear range.

It is known from theoretical investigations of SSI that rigid foundations are efficient in the scattering of incident seismic waves, and how this scattering depends on the foundation shape and its relative stiffness [9,18,29,34,56]. While this scattered energy is smaller for actual foundations of buildings, because those are never as rigid as their mathematical models [54], the scattering from flexible foundations still plays an important role in bringing about pockets of nonlinear soil deformation, which then lead to increased effective compliances and to their asymmetry. Observations of the response of full-scale structures during strong earthquake shaking show indirectly how prominent these nonlinearities in the soil structure systems can be [24,48–51]. Observations also show that these nonlinear deformations in the soil usually occur well before any damage begins in the buildings. Since this natural energy-absorbing mechanism is beneficial for reducing the damage in the buildings, it should be studied and whenever possible incorporated into future design methods.

Advanced large scale numerical simulations have been developed for analyses of dynamic response of soils, including nonlinear representation and complex geometry of foundations [7,26,58]. Large numerical models are necessary for engineering analyses in realistic setting, but detailed interpretation of some of their results becomes a challenge due to simultaneous action of their many complex features. With the aim of analyzing and interpreting only a subset of the phenomena, which accompany the nonlinear response of soil in the presence of soil–structure interaction, in this paper we choose only the most elementary representation of waves in the soil, and adopt the bi-linear yielding model for the soil. In calculations based on finite differences this then enables us to study times and places where strain localizations introduce permanent deformations in the soil. Our aim is to learn how the permanent deformations in the soil contribute to the absorption of incident seismic wave energy.

Nonlinear site response is a complex problem, which involves many geometrical and material parameters in the description of the governing models, where extrapolations are at best very difficult due to the chaotic nature of large excitation and large nonlinear response. Hence, in the following our modest goal will be merely to illustrate what may occur in the presence of nonlinearities in the soil and in the foundation during SSI, while the building remains linear. Comprehensive sensitivity studies of how these results depend on all governing parameters are beyond the scope of this paper.

2. Model

In general, during the wave passage, the soil, the foundation, and the superstructure can all undergo nonlinear deformations, and after the motion is over they can be left with permanent strains. Because the aim of this paper is to study only the nonlinear zones in the soil and in the foundation, the soil and the foundation will be modeled as nonlinear, while the building will be forced to remain linear. The three variants of the model to be considered are shown in Fig. 1a and b. The model in Fig. 1a will be considered twice, first with linear and then with nonlinear deformations in the foundation. The incoming wave is taken to be a half-sine pulse of a plane SH wave, which is intended to model strong-motion pulses observed in the ground motion near faults [19]. A dimensionless frequency $\eta = 2a/\lambda = a/(\beta_s t_{d0})$ will be used as a measure of the pulse duration (wavelength), where a is half the width of the foundation, λ is the wavelength of the incident wave, β_s is the shear-wave velocity in the soil, and t_{d0} is the duration of the pulse.

For completeness of this presentation, in the following we summarize briefly the finite difference model and its characteristics, following Gičev and Trifunac [15]. To set up the grid spacing in the finite difference representation of the model, the pulse is analyzed in space domain (s), and the displacement in the points occupied by the pulse is

$$w(s) = A \sin[(\pi s/(\beta_s t_{d0})] \tag{1}$$

where A is the amplitude of the pulse and s is the distance of the considered point to the wave front in initial time, in the direction of propagation. Using the fast Fourier transform, the half-sine pulse (Eq. (1)) is transformed into wave number domain (k) as follows:

$$w(k) = F[w(s)] \tag{2}$$

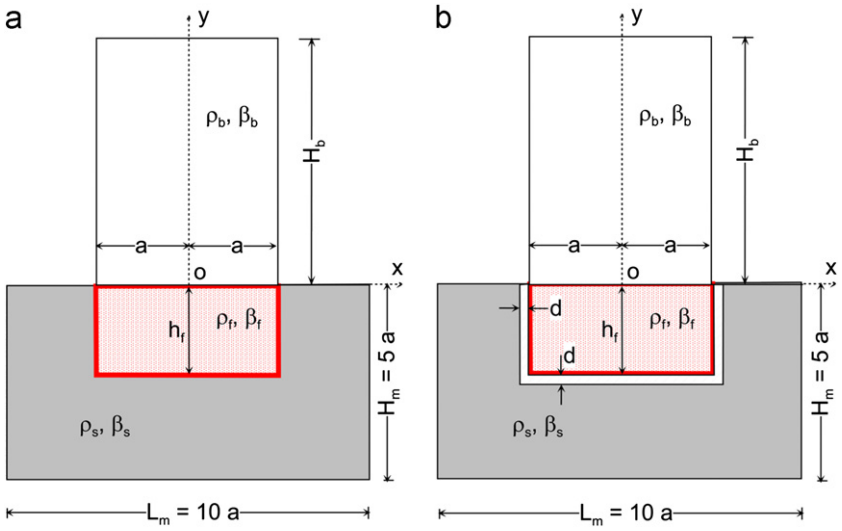

Fig. 1. Nonlinear soil–flexible foundation–linear structure system: (a) linear or nonlinear foundation and nonlinear soil and (b) foundation surrounded by soft, nonlinear layer ($d = h_f/10$) and nonlinear soil.

The maximum response occurs for $k=0$ (rigid-body motion). As k increases, the response decreases and diminishes towards zero as k approaches infinity. We selected the largest wave number to be considered in this analysis, $k=k_{max}$, for which the k-response is at least 0.03 of the maximum response [10]. Then, for this value of k_{max}, the corresponding wavelengths and the corresponding frequencies are

$$\lambda_{min}=2\pi/k_{max}=2\pi\beta/\omega_{max} \tag{3}$$

Accuracy of the finite difference (FD) grid depends on the ratio of the numerical and physical velocities of propagation, c/β, which ideally should be 1. The parameters that influence this accuracy are as follows: (1) the density of the grid $m=\lambda/\Delta x$ (m is the number of points per wavelength λ, and Δx is the spacing between the grid points); (2) the Courant number, $\chi=\beta_s\Delta t/\Delta x$; and (3) the angle of the wave incident, θ. It has been shown by Alford et al. [2], Dablain [5], and Fah [8] that the error increases when m decreases, χ decreases, and θ is close to 0 or $\pi/2$. For second-order approximation, the above authors recommend $m=12$.

To model soil response numerically, we chose a rectangular soil box with dimensions $L_m=10a$ and $H_m=L_m/2=5a$ (Fig. 1 ,b). For practical reasons, the maximum number of space intervals in the grid in the horizontal (x) direction is set at 250, and in the vertical (y) direction at 400 (125 in the soil box and 275 in the building). The minimum spatial interval for this setup is $\Delta x_{min}=L_m/250=95.5/250=0.382$ m. For a finer grid, the computational time increases rapidly. With this limitation in mind, and for $\eta=2$, the largest response is about 3% of the maximum response and has frequency $\omega_{max}=980$ rad / s [10]. From Eq. (3), the shortest wavelength is $\lambda_{min}=1.603$ m, and the finest grid density is $m=\lambda_{min}/\Delta x_{min}=1.603/0.382$. This corresponds to about 4 points / $\lambda_{min}<m_{min}$for this wavelength. Our numerical scheme is $O(\Delta t^2,\Delta x^2)$, so we need at least $m=12$ points/λ_{min} to resolve the shortest wavelength, λ_{min}. For $\eta=2$ our grid cannot resolve the shortest wavelength when we have only four spatial grid points. This implies that the pulse should be low-pass filtered. A cut-off frequency $\omega_c=200$ rad / s was chosen, and the pulse was low-pass filtered. This implies that $\lambda_{min}=7.854$ m and the grid density

$$m=\lambda_{min}/\Delta x_{min}=7.854/0.382\approx 20 \text{ points / } \lambda_{min}>m_{min} \tag{4}$$

It can be shown that for $\eta=0.5$ only a negligible amount of the total power is filtered out, while for $\eta=2$ a considerable amount is filtered out. Also, it can be shown that for $\eta=2$ the amplitude of the filtered pulse is smaller than the amplitude of the non-filtered pulse, which we chose to be $A=0.05$ m, while for $\eta=0.5$ the amplitude is almost equal to the amplitude of the non-filtered pulse [10]. Numerical tests have shown that the viscous absorbing boundary rotated towards the middle of the foundation–building interface reflects only a negligible amount of energy back into the model [9].

For 2-D problems, the numerical scheme is stable if the time increment [25] is

$$\Delta t\le \min[(1/\Delta x^2+1/\Delta y^2)^{1/2}\beta]^{-1} \tag{5}$$

We assume that the shear stress in the x direction depends only upon the shear strain in the same direction and is independent of the shear strain in the y direction. The motivation for this assumption comes from our simplified representation of layered soil, which is created by deposition (floods and wind) into more or less horizontal layers. The foundation and the soil are assumed to be ideally elasto-plastic, and the constitutive $\sigma-\varepsilon$ relationship is shown in Fig. 2. Further, it is assumed that the contact points between the soil and foundation remain bonded during the analysis and that the contact cells remain linear, as does the zone next to the artificial boundary (the bottom four rows and the left-most and right-most four columns of points in the soil box of Fig. 1a and b).

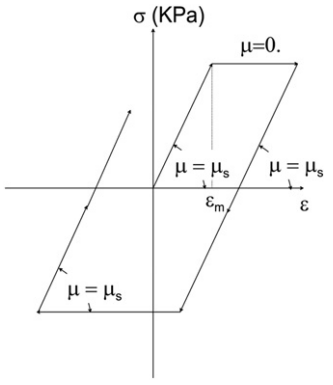

Fig. 2. Constitutive law, $\sigma-\varepsilon$, for the soil and foundation.

For our problem, the system of three partial differential equations (for u, v, and w) describing the dynamic equilibrium of an elastic body is reduced to one equation only (because $u=v=\partial/\partial z=0$). Neglecting the body forces in the z direction ($F_z=0$), this equation is

$$\rho\frac{\partial^2 w}{\partial t^2}=\left(\frac{\partial\tau_{xz}}{\partial x}+\frac{\partial\tau_{yz}}{\partial y}\right) \tag{6}$$

Introducing the new variables $v=\partial w/\partial t$, $\varepsilon_{xz}=\partial w/\partial x$ and $\varepsilon_{yz}=\partial w/\partial y$, and dividing Eq. (6) with ρ, the order (of six) is reduced to the system of three first-order partial differential equations:

$$\underline{U},_t=\underline{F},_x+\underline{G},_y, \tag{7}$$

where

$$\underline{U}=\begin{Bmatrix} v\\ \varepsilon_{xz}\\ \varepsilon_{yz}\end{Bmatrix}\ \underline{F}=\underline{F}(\underline{U})=\begin{Bmatrix}\frac{1}{\rho}\tau_{xz}\\ v\\ 0\end{Bmatrix}\ \underline{G}=\underline{G}(\underline{U})=\begin{Bmatrix}\frac{1}{\rho}\tau_{yz}\\ 0\\ v\end{Bmatrix} \tag{8}$$

The first equation in Eq. (7) is the dynamic equilibrium of forces in the z direction with neglected body force F_z. The second and third equations give the relations between the strains and the velocity. The abbreviations $\varepsilon_x=\varepsilon_{xz}$, $\sigma_x=\tau_{xz}$, $\varepsilon_y=\varepsilon_{yz}$, and $\sigma_y=\tau_{yz}$ will be used in the following. The Lax–Wendroff computational scheme [23] is used for solving Eq. (7) [9].

3. Energy and distribution of permanent strain

In the following examples, we use the properties of the Holiday Inn hotel in Van Nuys, California [3] to describe the building, and we consider the response in east–west (longitudinal) direction only. This building was studied extensively using different models and representations [11,13,20], and the body of those results can be used to complement future comparisons and interpretations of its response.

A question arises as to how to choose the yielding strain ε_m (Fig. 2) to study strain distribution in the system. The displacement, the velocity, and the linear strain in the soil ($\beta_s=250$ m/s) during the passage of a plane wave in the form of a half-sine pulse are

$$w=A\sin(\pi t/t_{d0}) \tag{9}$$

$$v=\dot{w}=(\pi/t_{d0})A\cos(\pi t/t_{d0}), \tag{10}$$

$$|\varepsilon| = v_{max}/\beta_s = \pi A/(\beta_s t_{d0}). \quad (11)$$

If, for a given input plane wave, we choose the yielding strain ε_m given by Eq. (11) multiplied by some constant between one and two, the strains in both directions will remain linear before the wave reaches the free surface or the foundation, for any incident angle. This case can be called "intermediate nonlinearity". If we want to analyze only the nonlinearity due to scattering and radiating from the foundation, we should avoid the occurrence of the nonlinear strains caused by reflection from the half-space boundary. Then we may choose $\varepsilon_m \geq \max(2\pi A \sin\gamma/\beta_s t_{d0}; 2\pi A \cos\gamma/\beta_s t_{d0})$. We call this case "small nonlinearity".

If the soil is allowed to undergo permanent strains due to wave passage of incident waves in the full space, then we may choose the maximum strain $\varepsilon_m < \max(\pi A \sin\gamma/\beta_s t_{d0}; \pi A \cos\gamma/\beta_s t_{d0})$. This condition guarantees that in either the x or y direction the soil will undergo permanent strains during the passage of the plane wave.

Generally, the yielding strain can be written as

$$\varepsilon_m = C v_{max}/\beta_s = C\pi A/(\beta_s t_{d0}) \quad (12)$$

where C is a constant that controls the yielding stress (strain) in the soil. We then consider the following cases of nonlinearity, depending upon C (see [15]):

- $C \geq 2$: Small nonlinearity. Permanent strain does not occur until the wave hits the foundation.
- $1 \leq C < 2$: Intermediate nonlinearity. Permanent strain does not occur until the wave is reflected from the free surface or is scattered from the foundation. Permanent strain will or will not occur after the reflection of the incident wave from the free surface, depending upon the angle of incidence.
- $C < 1$: Large nonlinearity. Permanent strain occurs after reflection from the free surface. Permanent strain may or may not occur before the wave reflects from the foundation surface.

4. Energy distribution in the system

The energy flow through a given area can be defined, in terms of a plane-wave approximation [1], as

$$E_{in}^{a} = \rho_s \beta_s A_{sn} \int_0^{t_{d0}} v^2 \, dt \quad (13)$$

where ρ_s and β_s are the density and shear-wave velocity in the soil and v is the particle velocity, which for the excitation considered in this paper is given by Eq. (10). A_{sn} is the area (normal to the direction of the ray) through which the wave is passing. For our geometrical setting (Fig. 1a, b), the area normal to the wave passage is

$$A_{sn} = 2H_m \sin\gamma + L_m \cos\gamma = L_m(\sin\gamma + \cos\gamma). \quad (14)$$

Inserting Eqs. (10) and (14) into (13) and integrating, the analytical solution for the input wave energy into the model is

$$E_{in}^{a} = \rho_s \beta_s L_m (\sin\gamma + \cos\gamma)(\pi A/t_{d0})^2 t_{d0}/2 \quad (15)$$

As can be seen from Eq. (15), for the defined size of the soil island, L_m, and the defined angle of incidence, γ, the input energy is reciprocal with the duration of the pulse, which means it is a linear function of the dimensionless frequency η. Because for short pulses in our example calculations are low-pass filtered up to $\omega_c = 200$ rad / s, the analytical and the numerical solutions (13) for input wave energy will not coincide.

Since our system is conservative, the input energy is balanced by the following:

- Cumulative energy going out from the model, E_{out}, computed using Eq. (13).

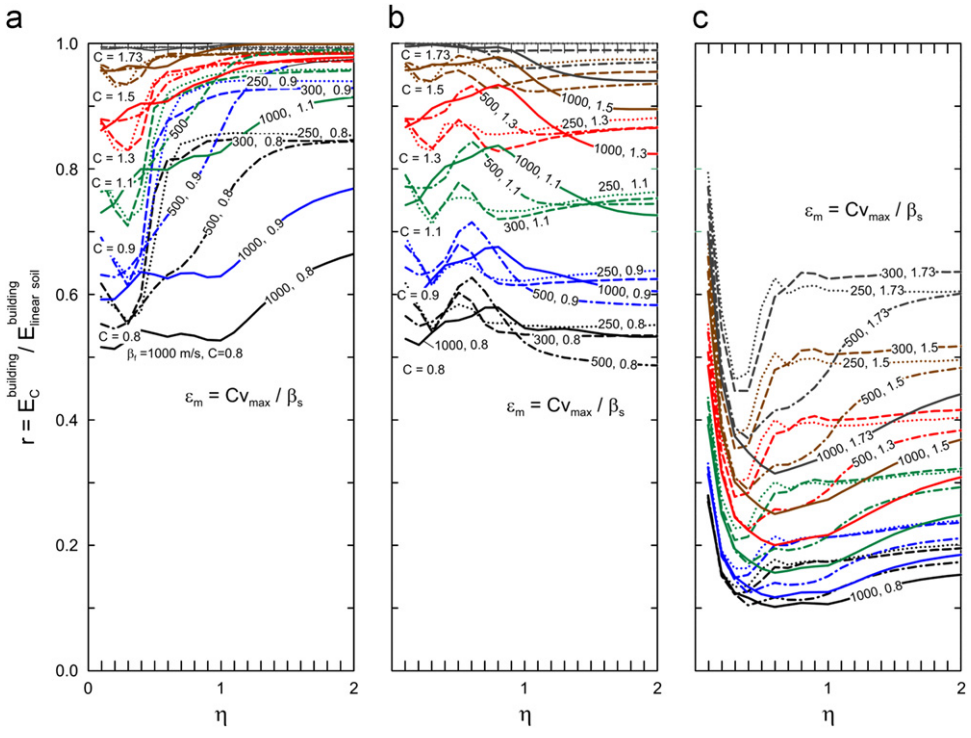

Fig. 3. Reduction of wave energy entering the linear building for (a) linear foundation, (b) nonlinear foundation, and (c) nonlinear, soft layer surrounding foundation ($d = h_f/10$; $\varepsilon_{yring} = \varepsilon_{ys}/5$), for different levels of soil nonlinearity (C=0.8, 0.9, 1.1, 1.3, 1.5, and 1.73) and for different foundation rigidities expressed via β_f =250, 300, 500, and 1000 m/s.

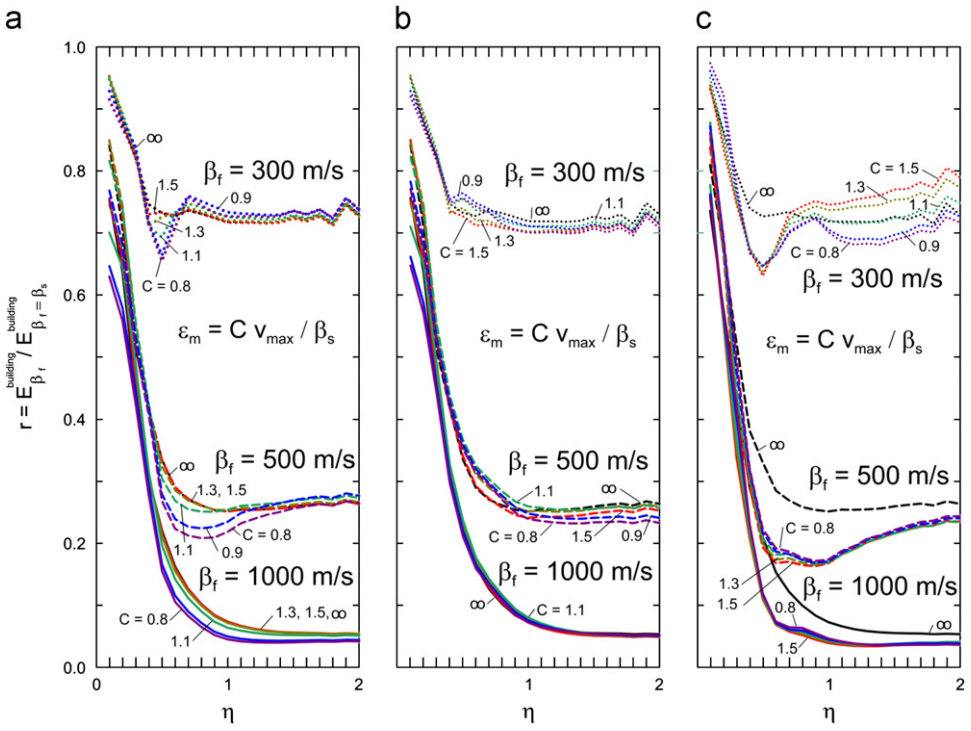

Fig. 4. Reduction of wave energy by scattering, entering the linear building for (a) linear foundation, (b) nonlinear foundation, and (c) foundation surrounded by soft, nonlinear layer, for different levels of soil nonlinearity (C=0.8, 0.9, 1.1, 1.3, 1.5, and ∞) and for different foundation rigidities expressed via β_f=300, 500, and 1000 m/s.

- Cumulative hysteretic energy (energy spent for creation and development of permanent strains in the soil), computed from:

$$E_{hys} = \sum_{t=0}^{T_{end}} \Delta t \sum_{i=1}^{N} \left(\sigma_{xi}(\Delta\varepsilon_{xpi} + 0.5\Delta\varepsilon_{xei}) + \sigma_{yi}(\Delta\varepsilon_{ypi} + 0.5\Delta\varepsilon_{yei})\right), \tag{16}$$

  where T_{end} is the time at the end of the analysis, N is the total number of points, σ_{xi},σ_{yi} are the stresses at the point i in the x and y directions, respectively, $\Delta\varepsilon_{xpi} = \varepsilon^{t+\Delta t}_{xpi} - \varepsilon^{t}_{xpi}$ is the increment of the permanent strain in the x direction at point i, and $\Delta\varepsilon_{ypi} = \varepsilon^{t+\Delta t}_{ypi} - \varepsilon^{t}_{ypi}$ is the increment of the permanent strain in the y direction at point i.
- Instantaneous energy in the building, consisting of kinetic and potential energies, which can be computed from

$$E_b = E_k + E_p = 0.5\Delta x\Delta y_b \sum_{i=1}^{N} \left(\rho v_i^2 + \mu(\varepsilon_x^2 + \varepsilon_y^2)\right) \tag{17}$$

This balance was discussed by Gičev [10] for a semi-cylindrical foundation, a pulse with $\eta = 1.5$, for incident angle $\gamma = 30^\circ$, and a yielding strain defined by C=1.5 (Eq. (12)), and it will be assumed to hold here as well for the rectangular foundation.

To study only the effect of scattering from the foundation, following Gičev [10] the building will be considered to be high enough so that the reflected wave from the top of the building cannot reach the building–foundation contact during the time of analysis. The analysis is terminated when the wave completely exits the soil island. In this paper, the hysteretic energy in the soil and the energy in the building are the subjects of interest. Gičev [10] studied these two types of energy as functions of the dimensionless frequency η. For a semi-circular foundation, he showed that as the foundation becomes stiffer, a larger part of the input energy is scattered, and less energy enters the building.

Fig. 3a–c shows the reduction of the energy entering the building relative to the case when the soil is linear. The results are shown for four different foundation stiffnesses expressed via β_f=250, 300, 500, and 1000 m/s. If the soil is linear, the reduction multiplier is 1. Fig. 3a is reproduced here from the work of Gičev and Trifunac [15] to help in the comparison with the results shown in Fig. 3b and c. It presents results for the foundation, which always deforms in the linear range. Fig. 3b shows the results for the foundation material allowed to deform nonlinearly. Fig. 3c shows the results for a nonlinear foundation surrounded by a thin, nonlinear layer (Fig. 1b).

In Fig. 3, we illustrate the energy reduction for six values of C=0.8, 0.9, 1.1, 1.3, 1.5, and 1.73, as follows for the case of nonlinear soil, linear foundation, and linear building (Fig. 3a): (1) For small nonlinearity (e.g., C=1.73), the ratios $E_C^{building}$ (C=1.73)/$E^{building}_{linear\ soil}$ ($C=\infty$) are close to one for every η, showing that the small nonlinearity in the soil does not reduce the energy entering the building significantly. (2) For intermediate nonlinearity (e.g., C=1.5), the ratios $E_C^{building}$ (C=1.5)/$E^{building}_{linear\ soil}$ ($C=\infty$) show that there is a small reduction of the energy entering the building with the smallest ratio $r\sim$0.94 near η=0.2–0.3 and for β_f=250 m/s in Fig. 3a. The values of η=0.2–0.3 correspond to the excitation with wavelengths 3–5 times longer than the width of the foundation, and this corresponds to the cases in which all points along the contact of soil and foundation are forced to move in phase and with similar amplitudes. With increasing η (larger than $\sim$0.7), the reduction decreases and the ratio r in Fig. 3a tends towards 1. (3) For big nonlinearity (e.g., C=0.8), the ratios $E_C^{building}$ (C=0.8)/$E^{building}_{linear\ soil}$ ($C=\infty$) show that the reduction of energy entering the building is significant for all considered values of foundation stiffness. The ratio r is the smallest for the stiffest considered foundation (β_f=1000 m/s). Fig. 3b shows that when the foundation experiences nonlinear deformations, the reduction of the high frequency energy entering the building is further increased relative to the case when the foundation remains linear. Fig. 3c shows significant energy absorption capacity of thin nonlinear layer surrounding the foundation.

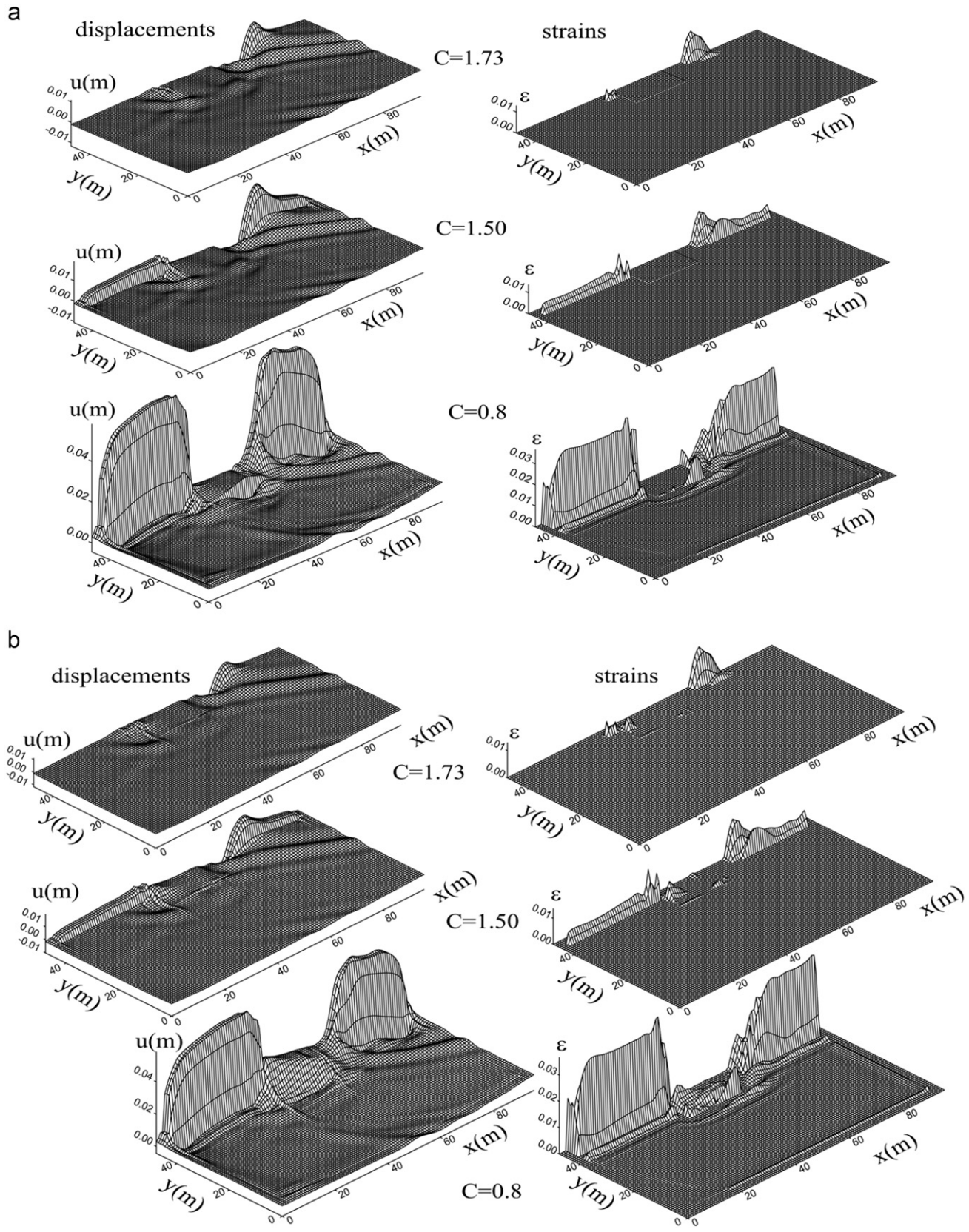

Fig. 5. (a) Model with nonlinear soil, linear foundation, and linear building. Permanent displacements and strains in soils with small ($C=1.73$), intermediate ($C=1.5$), and large nonlinearity ($C=0.8$). The angle of incidence is $\gamma=\pi/6(30^\circ)$, amplitude of the pulse $A=0.05$ m, and the dimensionless frequency $\eta=h_f/(\beta_s t_d)=1.5$, where h_f is the foundation height. The properties (SH wave velocity, density, width, and height) for the media are nonlinear soil (250 m/s, 2000 kg/m^3, ∞, ∞), yielding strain $\varepsilon_m=C v_{max}/\beta_s$, linear rectangular foundation (500 m/s, 2000 kg/m^3, 19.1 m, 9.55 m), linear building (100 m/s, 270 kg/m^3, 19.1 m, 20.03 m). (b) Model with nonlinear soil, nonlinear foundation, and linear building. Permanent displacements and strains in soils with small ($C=1.73$), intermediate ($C=1.5$) and large nonlinearity ($C=0.8$). The angle of incidence is $\gamma=\pi/6(30^\circ)$, amplitude of the pulse $A=0.05$ m, and the dimensionless frequency $\eta=h_f/(\beta_s t_d)=1.5$, where h_f is the foundation height. The properties (SH wave velocity, density, width, and height) for the media are nonlinear soil (250 m/s, 2000 kg/m^3, ∞, ∞), yielding strain $\varepsilon_m=C v_{max}/\beta_s$, nonlinear rectangular foundation (500 m/s, 2000 kg/m^3, 19.1 m, 9.55 m), yielding strain $\varepsilon_{yf}=\varepsilon_m G_s/G_f$, linear building (100 m/s, 270 kg/m^3, 19.1 m, 20.03 m). (c) Model with nonlinear soil, nonlinear foundation, soft layer surrounding the foundation, and linear building interaction. Permanent displacement and strain in soil with small ($C=1.73$), intermediate ($C=1.5$) and large nonlinearity ($C=0.8$). The angle of incidence $\gamma=\pi/6(30^\circ)$, the amplitude of the pulse $A=0.05$ m, and the dimensionless frequency $\eta=h_f/(\beta_s t_d)=1.5$, where h_f is the foundation height. The properties (SH wave velocity, density, width, height) for the media are nonlinear soil (250 m/s, 2000 kg/m^3, ∞, ∞). Yielding strain $\varepsilon_m=C v_{max}/\beta_s$, nonlinear soil ring around the foundation with thickness $h_f/10$ and yielding strain $\varepsilon_{yring}=\varepsilon_{ys}/5$, nonlinear rectangular foundation (500 m/s, 2000 kg/m^3, 19.1 m, 9.55 m), yielding strain $\varepsilon_{yf}=\varepsilon_m G_s/G_f$, linear building (100 m/s, 270 kg/m^3, 19.1 m, 20.03 m).

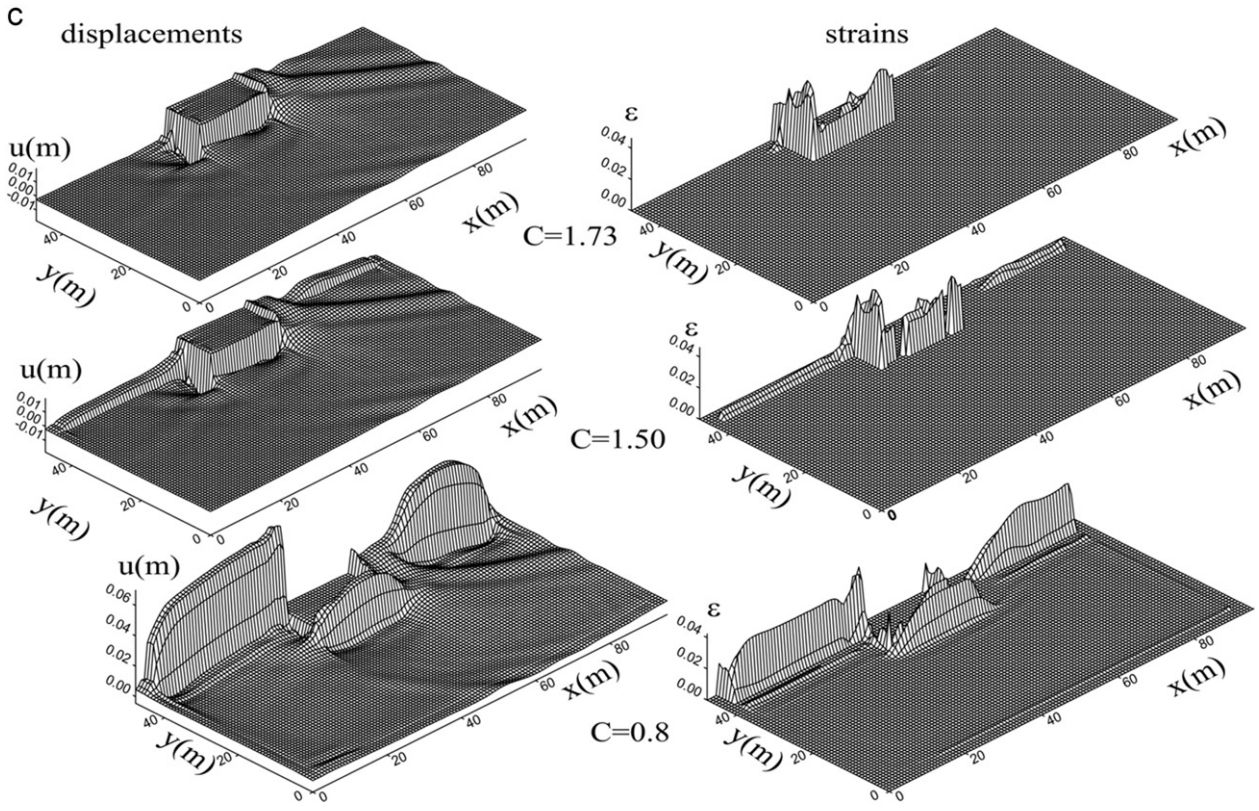

Fig. 5. (*continued*)

The results computed for case (3) above are dependent upon the size of the model box. Before the wave reaches the foundation, it loses energy due to work spent for creation of permanent strains in the soil. But for our examples, this dependence turns out to be small. For example, as pointed out in Gičev and Trifunac [15], for $\beta_f=250$ m/s and $\eta=0.3$, the case of linear soil gives $E^{building}_{linearsoil}=164{,}540$ J. For soil box $L_m=10a$ wide and $H_m=5a$ deep, the energy entering the building is $E^{building}_{C}$ $(C=0.8)=90{,}769$ J, and the ratio $r=0.55$. For a soil box $L_m=20a$ wide and $H_m=10a$ deep, the energy entering the building is $E^{building}_{C}(C=0.8)=88{,}884$ J, and $r=0.54$, which is about a 2% difference for an approximately 2×2 smaller soil box. From this, one can conclude that if this extreme case $r_{\beta_f=250}(C=0.8,\eta=0.3)=r^{min}_{\beta_f=250}(C=0.8,\eta)$ (Fig. 3a) gives only a 2% difference, at other values of η we will obtain even smaller differences due to different sizes of the model. However, if C becomes smaller (for larger nonlinearities) the dependence on the model size will become more pronounced.

Next, we illustrate how the level of the nonlinearity affects the level of scattering. This is shown in Fig. 4a–c. It is seen that the scattering does not depend much on the level of nonlinearity in the soil for small and intermediate nonlinearities and is essentially the same as in the case of linear soil. For large nonlinearity, the effect becomes more significant. The examples in Fig. 4 show that the stiffness of the foundation is the key factor, which determines how much energy is scattered from the foundation.

Fig. 5a–c illustrates the permanent displacements (left) and strains (right) in the soil for nonlinear soil, linear (a) or nonlinear (b) foundation, (c) nonlinear foundation surrounded by a thin layer of nonlinear soil, and linear building. The figure shows permanent displacements (left) and strains (right) in the foundation and the soil with small ($C=1.73$), intermediate ($C=1.5$), and large nonlinearities ($C=0.8$). The angle of wave incidence is $\gamma=\pi/6$ (30°), the amplitude of the pulse is $A=0.05$ m, and the dimensionless frequency is $\eta=h_f/(\beta_s t_d)=1.5$. In all examples, the foundation depth is equal to its half width, $h_f=a$. The properties for the three media (SH wave velocity, density, width, height) are in nonlinear soil (250 m/s, 2000 kg/m^3, ∞, ∞), yielding strain $\varepsilon_m=Cv_{max}/\beta_s$; in a linear or nonlinear rectangular foundation (500 m/s, 2000 kg/m^3, 19.1 m, 9.55 m), where h_f is foundation height, and in a linear building (100 m/s, 270 kg/m^3, 19.1 m, 20.03 m).

Along the model boundaries (four columns and four rows in the FD mesh), both displacements and strains decrease due to gradual transition from nonlinear to linear material properties in the model.

5. Flexible foundation

The 1D nature of the building response on the rigid foundation eliminates the possibility to excite torsion in the building (rotation about the vertical y-axis in Fig. 1) due to wave passage effects, and for all incident angles of the wave, γ. However, the wave passage along the base of the building for flexible foundation deforms the building as the wave propagates along the foundation width. For long waves, this excitation of the building can be viewed as out of plane motion combined with torsion of the base. We illustrate this by computing the cord rotation between the two corner points at the base of the building (points A and B). We illustrate this cord rotation versus time in Fig. 6, for the case of nonlinear soil and linear but deformable foundation. As would be expected this "torsion" becomes small and approaches zero as β_f increases. For the model parameters chosen in this paper, this torsion also decreases with increasing nonlinearity in the soil response, and is largest for linear soil response.

The wave passage along the base of the building will increase the vertical strains, at the base of the building, particularly near corners (points A and B) and will result in their time and space

variations. This increase will depend on the relative stiffness of the building in translation and in torsion, and on the horizontal wave length of the motion propagating from the foundation into the building [27,28]. A related discrete model of a rigid "building" on multiple columns suggests that this amplification can be considerable [21]. We illustrate this qualitatively in Fig. 7, at the time when the wave begins to enter the building. We show the amplitudes of vertical strain in a narrow zone above and below the building foundation interface. It is seen that while the presence of nonlinear response in the soil, and scattering of incident waves from the flexible foundation contribute to the reduction of seismic wave energy entering the building, the building excitation and its response become more complex and require analysis in terms of more degrees of freedom.

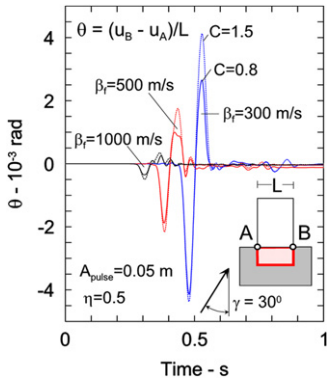

Fig. 6. Cord rotations, between points A and B on the building–foundation interface, for intermediate nonlinearity in the soil ($C=1.5$), for large nonlinearity in the soil ($C=0.8$), and for linear deformations in the foundation.

6. Discussion and conclusions

The examples of nonlinear soil and foundation responses shown in this paper confirm that the energy entering a building can be reduced significantly before the waves approach and then enter the building. Nonlinear soil deformations are thus a far more efficient "base isolation" system than what can be accomplished by installing base isolators at the foundation level or somewhere within the structure. Clearly, it is better (a) to absorb energy before it enters the foundation and the structure, and (b) to absorb it in the soil, which has far more powerful absorbing capacity that any isolator because it can accommodate large volumes with nonlinear deformations. Finally, the energy absorption by nonlinear soil response is cheap and maintenance free.

Nature has already provided us with such a powerful base isolation system, as evidenced by the documented reduction of damage to the buildings during the 1994 Northridge [45] and 1933 Long Beach earthquakes [36]. Such reductions obviously also occurred during many other earthquakes in spite of the fact

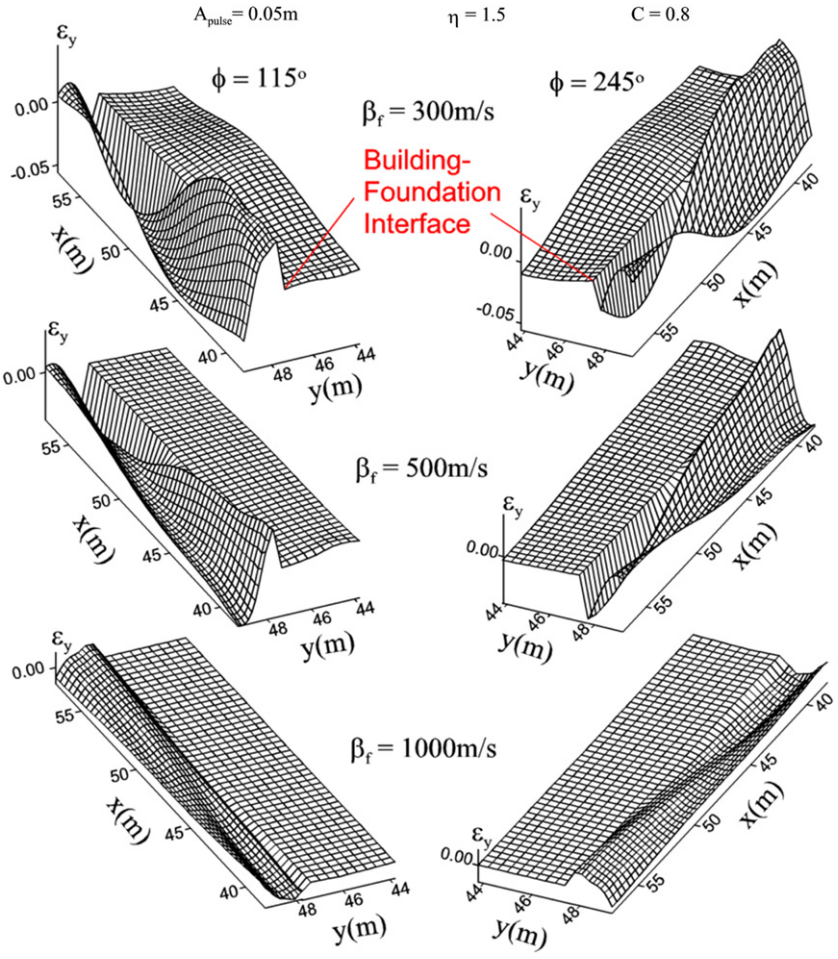

Fig. 7. Distribution of vertical strains ε_y in the narrow strips above and below the building foundation interface, for $\eta=1.5$ and large nonlinear response in the soil ($C=0.8$), different rigidities of the foundation expressed via shear wave velocity ($\beta_f=300$, 500 and 1000 m/s), and for linear deformations of the foundation. Two views are shown for $\phi=115^\circ$ and 245°, measured clockwise from the vertical axis pointing down.

that those may not have been documented. However, as for any other energy-absorbing system, the natural soil can also be an efficient and controllable energy sink only for a range of excitation amplitudes. This range will depend on many local conditions, and on the proximity to the moving fault and to the zones of extreme amplification of seismic waves. In terms of what has been learned following the Northridge earthquake, this useful range might extend to peak ground velocities of 150–200 cm/s [45]. Near and beyond these large, strong motion amplitudes, the soil may begin to break into blocks, moving independently on the liquefied substratum. The structures will then begin to be damaged and destroyed by large differential displacements [44] and rotations of their foundation, due to deformations and forces larger than those resulting from shaking.

In a real three-dimensional setting, the nonlinear soil response is obviously far more complex than what has been illustrated in this paper, but the effects can be expected to be qualitatively the same. The challenge for the next generation of performance-based design methods will be to include the soil in the design of the complete building-soil system and to maximize its energy-absorption potential for incident strong-motion waves.

Acknowledgments

We are grateful and acknowledge the suggestions made by two reviewers, whose comments resulted in significant improvements of this paper.

References

[1] Aki K, Richards P. Quantitative seismology, theory and methods. San Francisco: W.H. Freeman & Co.; 1980.
[2] Alford RM, Kelly KR, Boore DM. Accuracy of finite-difference modeling of the acoustic wave equation. Geophysics 1974;39:834–42.
[3] Blume et al.. Holiday Inn, in San Fernando, California, earthquake of February 9, 1971. In: Murphy LM, editor. Washington, DC: US Department of Commerce, National Oceanic and Atmospheric Administration; 1973.
[4] Chin BH, Aki K. Simultaneous study of the source, path and site effects on strong ground motion during the Loma Prieta earthquake: a preliminary result on pervasive nonlinear site effects. Bulletin of the Seismological Society of America 1991;81:1859–84.
[5] Dablain MA. The application of high-order differencing to the scalar wave equation. Geophysics 1986;51(1):54–66.
[6] Duke CM. Bibliography of effects of soil conditions on earthquake damage. Berkeley, CA: Earthquake Engineering Research Institute; 1958.
[7] Elgamal A, Linjun Y, Zaohui Y, Conte JP. Three-dimensional seismic response of humboldt bay bridge-foundation-ground system. Journal of Structural Engineering—ASCE 2008;134(7):1165–76.
[8] Fah DJ. A hybrid technique for the estimation of strong ground motion in sedimentary basins. Dissertation. Zurich, Switzerland: Swiss Federal Institute of Technology; 1992.
[9] Gičev V. Investigation of soil–flexible foundation–structure interaction for incident plane SH waves. Ph.D. Dissertation. Department of Civil Engineering, Los Angeles, CA: University of Southern California; 2005.
[10] Gičev V. Soil–structure interaction in nonlinear soil. Izgradnja 2008;62(12): 555–66.
[11] Gičev V, Trifunac MD. Energy and power of nonlinear waves in a seven story reinforced concrete building. Indian Society of Earthquake Technology 2007; vol. 44(1): 305–323. Available from: 〈http://home.iitk.ac.in/~vinaykg/iset.html〉.
[12] Gičev V, Trifunac MD. Transient and permanent shear strains in a building excited by strong earthquake pulses. Soil Dynamics and Earthquake Engineering 2009;29(10):1358–66.
[13] Gičev V, Trifunac MD. Rotations in a shear beam model of a seven-story building caused by nonlinear waves during earthquake excitation. Structural Control and Health Monitoring 2009;16(4):460–82.
[14] Gičev V, Trifunac MD. Transient and permanent rotations in a shear layer excited by strong earthquake pulses. Bulletin of the Seismological Society of America 2009;99(2B):1391–403.
[15] Gičev V. Trifunac MD. Asymmetry of nonlinear soil strains during soil-structure interaction excited by SH pulse. Izgradnja 2012;66(5–6):252–68.
[16] Gupta ID, Trifunac MD. Order statistics of peaks in earthquake response. Journal of Engineering Mechanics—ASCE 1988;114(10):1605–27.
[17] Gupta ID, Trifunac MD. Statistics of ordered peaks in the response of non-classically damped structures. Probabilistic Engineering Mechanics 1999;14(4): 329–37.
[18] Hayir A, Todorovska MI, Trifunac MD. Antiplane response of a dike with flexible soil–structure interface to incident SH waves. Soil Dynamics and Earthquake Engineering 2001;*21*:603–13.
[19] Housner GW, Trifunac MD. Analysis of accelerograms—Parkfield earthquake. Bulletin of the Seismological Society of America 1967;57(6):1193–220.
[20] Ivanović SS, Trifunac MD, Novikova EI, Gladkov AA, Todorovska MI. Ambient vibration tests of a seven-story reinforced concrete building in Van Nuys, California, damaged by the 1994 Northridge earthquake. Soil Dynamics and Earthquake Engineering 2000;19(6):391–411.
[21] Jalali RS, Trifunac MD. A note on the wave-passage effects in out-of-plane response of long structures to strong earthquake pulses. Soil Dynamics and Earthquake Engineering 2011;31(4):640–7.
[22] Kanai K. Engineering seismology. Tokyo: University of Tokyo Press; 1983.
[23] Lax PD, Wendroff B. Difference schemes for hyperbolic equations with high order of accuracy. Communications on Pure and Applied Mathematics, 1964;XVII: 381–98.
[24] Luco JE, Trifunac MD, Wong HL. On the apparent changes in dynamic behavior of a nine-story reinforced concrete building. Bulletin of the Seismological Society of America 1987;77(6):1961–83.
[25] Mitchell AR. Computational methods in partial differential equations. New York: John Wiley & Sons; 1969.
[26] Prevost JH. Nonlinear dynamic response analysis of soil and soil–structure interaction systems, seminar on soil dynamics and geotechnical earthquake engineering. In: Seco E, Pinto P, editors. Soil dynamics and earthquake engineering. Rotterdam: Balkema; 1993. p. 49–126.
[27] Todorovska MI, Trifunac MD. Antiplane earthquake waves in long structures. Journal of Engineering Mechanics—ASCE 1989;115(12):2687–708.
[28] Todorovska MI, Trifunac MD. A note on excitation of long structures by ground waves. Journal of Engineering Mechanics—ASCE 1990;116(4):952–64.
[29] Todorovska MI, Trifunac MD. The effects of wave passage on the response of base-isolated buildings on rigid embedded foundations. Report CE 93-10, Los Angeles, California: Department of Civil Engineering, University of Southern California; 1993. Available from: 〈http://www.usc.edu/dept/civil_eng/Earthquake_eng/〉.
[30] Todorovska MI, Trifunac MD. Distribution of pseudo spectral velocity during Northridge, California Earthquake of 17 January, 1994. Soil Dynamics and Earthquake Engineering 1997;16(3):173–92.
[31] Todorovska MI, Trifunac MD. Amplitudes, polarity and time of peaks of strong ground motion during the 1994 Northridge, California earthquake. Soil Dynamics and Earthquake Engineering 1997;16(4):235–58.
[32] Todorovska MI, Trifunac MD. Discussion of the role of earthquake hazard maps in loss estimation: a study of the northridge earthquake, by R.B. Olshansky. Earthquake Spectra 1998;14(3):557–63.
[33] Todorovska MI, Trifunac MD. Liquefaction opportunity mapping via seismic wave energy. Journal of Geotechnical and Geoenvironmental Engineering—, ASCE 1999;125(12):1032–42.
[34] Todorovska MI, Hayir A, Trifunac MD. Antiplane response of a dike on flexible embedded foundation to incident SH-waves. Soil Dynamics and Earthquake Engineering 2001;21:593–601.
[35] Trifunac MD. Empirical criteria for liquefaction in sands via standard penetration tests and seismic wave energy. Soil Dynamics and Earthquake Engineering 1995;14(6):419–26.
[36] Trifunac MD. Nonlinear soil response as a natural passive isolation mechanism, paper II—the 1933, Long Beach, California earthquake. Soil Dynamics and Earthquake Engineering 2003;23(7):549–62.
[37] Trifunac MD. Power design method. In: Proceedings of the earthquake engineering in the 21st century to mark 40th anniversary of IZIIS—Skopje. Skopje and Ohrid, Macedonia; August 28–September 1 2005.
[38] Trifunac MD. The nature of site response during earthquakes. In: Proceedings of the NATO ARW workshop in Borovec, T. Schantz and R.Iankov editors, NATO science for piece and security series C: environmental security. Springer Science+Business Media, B. V; 2009. p. 3–31.
[39] Trifunac MD, Ivanović SS. Reocurrence of site specific response in former Yugoslavia—Part I: Montenegro. Soil Dynamics and Earthquake Engineering 2003;23(8):637–61.
[40] Trifunac MD, Ivanović SS. Reoccurrence of site specific response in former Yugoslavia—Part II: Friuli, Banja Luka and Kopaonik. Soil Dynamics and Earthquake Engineering 2003;23(8):663–81.
[41] Trifunac MD, Todorovska MI. Nonlinear soil response—1994 Northridge California, earthquake. Journal of Geotechnical Engineering—ASCE 1996;122(9): 725–35.
[42] Trifunac MD, Todorovska MI. Northridge, California, earthquake of 1994: density of red-tagged buildings versus peak horizontal velocity and intensity of shaking. Soil Dynamics and Earthquake Engineering 1997;16(3):209–22.
[43] Trifunac MD, Todorovska MI. Northridge, California, earthquake of 17 January 1994: density of pipe breaks and surface strains. Soil Dynamics and Earthquake Engineering 1997;16(3):193–207.
[44] Trifunac MD, Todorovska MI. Response spectra and differential motion of columns. Earthquake Engineering and Structural Dynamics 1997;26(2): 251–68.
[45] Trifunac MD, Todorovska MI. Nonlinear soil response as a natural passive isolation mechanism—The 1994 Northridge, California, earthquake. Soil Dynamics and Earthquake Engineering 1998;17(1):41–51.

[46] Trifunac MD, Todorovska MI. 1971 San Fernando and 1994 Northridge, California, earthquakes: did the zones with severely damaged buildings reoccur? Soil Dynamics and Earthquake Engineering 2004;24(3):225–39.
[47] Trifunac MD, Hao TY, Todorovska MI. On reoccurrence of site specific response. Soil Dynamics and Earthquake Engineering 1999;18(8):569–92.
[48] Trifunac MD, Hao TY, Todorovska MI. On energy flow in earthquake response. Report CE 01-03. Department of Civil Engineering, University of Southern California; 2001.
[49] Trifunac MD, Ivanović SS, Todorovska MI. Apparent periods of a building I: Fourier analysis. Journal of Structural Engineering—ASCE 2001;127(5):517–26.
[50] Trifunac MD, Ivanović SS, Todorovska MI. Apparent periods of a building II: time–frequency analysis. Journal of Structural Engineering—ASCE 2001;127(5): 527–37.
[51] Trifunac MD, Todorovska MI, Hao TY. Full-scale experimental studies of soil–structure interaction—a review. In: Proceedings of the 2nd US–Japan workshop on soil–structure interaction. Tsukuba City, Japan (CD available from Building Research Institute of Japan, Tsukuba City, Japan); 2001. p. 52.
[52] Trifunac MD, Todorovska MI, Ivanović SS. A note on distribution of uncorrected peak ground accelerations during the Northridge, California, earthquake of 17 January 1994. Soil Dynamics and Earthquake Engineering 1994;13(3):187–96.
[53] Trifunac MD, Todorovska MI, Ivanović SS. Peak velocities, and peak surface strains during Northridge, California, earthquake of 17 January 1994. Soil Dynamics and Earthquake Engineering 1996;15(5):301–10.
[54] Trifunac MD, Ivanović SS, Todorovska MI, Novikova EI, Gladkov AA. Experimental evidence for flexibility of a building foundation supported by concrete friction piles. Soil Dynamics and Earthquake Engineering 1999;18(3):169–87.
[55] Udwadia FE, Trifunac MD. Characterization of response spectra through statistics of oscillator response. Bulletin of the Seismological Society of America 1974;64(1):205–19.
[56] Wong HL, Trifunac MD. Interaction of a shear wall with the soil for incident plane sh-waves: elliptical rigid foundation. Bulletin of the Seismological Society of America 1974;64(6):1825–42.
[57] Yu G, Anderson JG. On the characteristics of nonlinear soil response. Bulletin of the Seismological Society of America 1993;83(1):218–44.
[58] Zhang Y, Conte JP, Yang Z, Elgamal A, Bielak J, Acero G. Two-dimensional nonlinear earthquake response analysis of bridge–foundation–ground system. Earthquake Spectra 2008;24(2):343–86.